The Holocene 19,1 (2009) pp. 129–142

An evolutionary model for the Holocene formation of the Pearl River delta, China

Y. Zong,[1]* G. Huang,[2] A.D. Switzer,[1] F. Yu[3] and W.W.-S. Yim[1]

([1]Department of Earth Sciences, The University of Hong Kong, Hong Kong Special Administration Region, China; [2]College of Environmental Science and Engineering, South China University of Technology, Guangzhou, P.R. China; [3]Department of Geography, University of Durham, Durham, UK)

Received 9 April 2008; revised manuscript accepted 17 June 2008

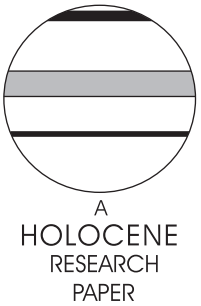

Abstract: This paper reconstructs the evolutionary history of the Pearl River delta over the last 9000 years and investigates land–sea interaction in a large deltaic complex which formed under the influence of Asian monsoon climate. Specifically, this research examines the delta evolution in the context of three driving mechanisms: (1) rising sea level that influences the available accommodation space, (2) fluvial discharge as influenced by monsoon climate and (3) human activities that alter sedimentation within the deltaic system. Results reveal that the formation of deltaic sequences was initiated as a consequence of rapid sea-level rise between 9000 and 7000 cal. yr BP. The rate of sea-level rise slowed down markedly around 7000 cal. yr BP and sedimentation switched from transgressive to regressive. Initially, both the progradation of the delta plains near the apex and aggradation of delta front sedimentation in the central and lower parts of the receiving basin were fast owing to strong monsoonal-driven runoff. The progradation rate gradually slowed down between 6800 and 2000 cal. yr BP as monsoonal-driven runoff weakened. Rapid shoreline advances during the last 2000 years were the result of significantly increased human activities, a practice that trapped sediments in the encircled tidal flats along the front of delta plains. The evolutionary history of the Pearl River delta demonstrates the interplay between the three driving mechanisms.

Key words: Sea-level change, monsoonal runoff, human activities, Holocene, deltaic landforms, coastal evolution.

Introduction

Deltas are dynamic and actively evolving landforms that occur at the mouths of river systems where sediments are deposited as they enter the sea or other large water body. The formation of deltaic landforms is influenced by a number of driving mechanisms, particularly sea-level change, fluvial processes and human activities. A number of large deltas formed during the Holocene in East and Southeast Asia at river mouths have received large quantity of sediments (Woodroffe *et al*., 2006). The initiation of modern coastal deltas is a result of the eustatic rise in sea level that controlled the base level of the available accommodation space for a delta to evolve (Stanley and Warne, 1994). The rapid rise in sea level during the early Holocene has resulted in deposition of transgressive estuarine sequences, whilst the relatively stable sea level during the middle and late Holocene has led to the formation of regressive deltaic systems. Since sea level reached an altitude close to present height about 7000 years ago, fluvial and coastal processes have become important controlling factors in the evolutionary history of deltas (Woodroffe, 2000; Chen *et al*., 2007). During this period, the evolutionary history of large deltas has been influenced by changes in sediment supply, certainly in the cases of the Yangtze delta (Hori *et al*., 2001; Saito *et al*., 2001), the Song Hong River delta (Tanabe *et al*., 2006), the Mekong delta (Nguyen *et al*., 2000; Ta *et al*., 2002), the Chao Phraya delta of Thailand (Tanabe *et al*., 2003) and the Ganges-Brahmaputra delta (Goodbred and Kuehl, 2000). However, in these cases, the impact of human activities on deltaic landform evolution has rarely been investigated in much detail.

The morphological characteristics of any coastal delta are determined by the interaction of numerous factors including the antecedent geomorphology of the receiving basin, tidal regime, wave energy and coastal currents. In some cases, the morphological characteristics of deltaic landforms change as a result of alterations in the hydrological conditions in the receiving basins. For instance, the morphological development of the Mekong delta resulted in changes from fluvial-tidal-dominated to wave-dominated formations about 3000 years ago (Nguyen *et al*., 2000). Similar changes are recorded also from the Han River delta (Zong, 1992) and the Song Hong River delta (Tanabe *et al*., 2003). However, the dominant processes in deltas such as the Yangtze (Hori *et al*., 2001) and the Ganges-Brahmaputra (Goodbred and Kuehl, 2000) have not changed since about 6000 years ago. In other words, we need to analyse the morphological characteristics of each delta in connection with its local geomorphology and hydrological conditions.

Changes of deltaic shoreline position and landscape function in the near future have become important topics of socioeconomic concern, particularly under the scenarios of global warming and

*Author for correspondence (e-mail: yqzong@hkucc.hku.hk)

 10.1177/0959683608098957

sea-level rise. This is particularly important in Asia where many deltas host dense human population and/or diverse fauna and flora. To predict future changes, we must improve our understanding of what has occurred in the past and what is happening at present. In this study, the Pearl River delta is examined with the aim of defining the Holocene history of the deltaic evolution with particular attention to the interplay between major driving mechanisms. Past surveys in the delta (eg, Huang *et al*., 1982) have provided a good lithological framework in which the deltaic evolutionary history can be placed and examined. Additionally, human activities in the delta have been intense in the past 2000 years (Li *et al*., 1990), which presents a good case study for the examination of human impacts on the deltaic evolutionary history. The research objectives are therefore two-fold. The first is to establish present-day sedimentary characteristics from delta plain to pro-delta environments in order to help interpretation of palaeoenvironments that are based on the examination of sedimentary cores and microfossils. The second is to reconstruct the stages of deltaic landform formation, and present a model for the evolutionary history of the Pearl River delta that explains the interplay between the driving mechanisms – sea-level change, monsoonal-driven fluvial runoff and human activities.

Study area

Geologically, the Pearl River drainage basin formed as a result of uplift of the Tibetan Plateau during the Tertiary and Quaternary periods, lagging considerably behind the continent/continent collision of ~34 million years ago (Aitchison *et al*., 2007). Before the late Quaternary, sediments from the river system bypassed the current deltaic basin and were deposited on the northern continental shelf and slope of the South China Sea. Active faulting during the late Quaternary resulted in land subsidence and the development of a broad receiving basin, into which a sequence of terrestrial sediments were deposited and now overlie a bedrock basement of Cretaceous–Tertiary sandstones and Mesozoic granites (Huang *et al*., 1982). In much of the basin two late-Quaternary deltaic sequences, separated by a terrestrial unit, were deposited in the receiving basin. The older deltaic sequence formed during the last interglacial when sea level was at least as high as present (Yim, 1994). The younger deltaic sequence was deposited during the present interglacial.

The Pearl River is the general name for the three large rivers (the East, the North and the West, see Figure 1A) that flow into the receiving basin and have produced two delta plains before entering the South China Sea. The North and West Rivers are separated by a row of rocky islands and they merge in the central part of the receiving basin (Figure 1B). The river catchment lies along the 23.5°N parallel and is relatively small in comparison with the Yangtze and Mekong (Table 1). The Pearl River is 2214 km in length (the West River), and it drains an area of 425 700 km^2. At present the receiving basin is not completely filled and drains into a large estuary of about 1740 km^2. The estuary separates two deltaic plains that cover about 5650 km^2, excluding 2360 km^2 of rocky islands (Table 1). The upper estuary, north of Humen (Figure 1B), is about 2.5 km wide. The width of the lower estuary between Humen and Macau/Hong Kong varies between 24 km and 30 km. The estuary is protected from storm waves by a cluster of rocky offshore islands. The main modern tidal channel runs directly south from the upper estuary and incises to about 10 m deep at the mouth between Hong Kong and Macau (Figure 1B). A secondary tidal channel runs southeast, through Hong Kong, and turns south into the South China Sea.

The Pearl River catchment basin is under a monsoonal climate (An, 2000). At present the annual average precipitation is between 1600 and 2000 mm/yr, but over 80% of rainfall occurs during spring and summer, indicative of a warm humid summer and a dry cool winter. The annual average temperature is around 22°C. The warm and humid conditions over the catchment support tropical to subtropical mixed evergreen and deciduous forests. Chemical weathering is the dominant weathering process that acts on exposed bedrock. The variability of the monsoon climate causes considerable contrast in seasonal and interannual water discharge from as low as 2000 m^3/s in a dry winter to as high as 46 300 m^3/s recorded in a 100-yr flood event (Huang *et al*., 2004). The annual average runoff is reported as 5663 m^3/s (Xu *et al*., 1985). On average, the Pearl River discharges 302 000 $\times 10^6$ m^3 of water and 83.4 $\times 10^6$ tonnes of suspended sediment a year (Table 1). The sediment load in the Pearl River (0.276 kg/m^3 on average) is, however, the lowest among large Asian rivers (Table 1). More than 90% of sediment comes from the West and North Rivers. Offshore currents during winter seasons predominantly carry sediment westwards. As a result, the eastern side of the estuary, particularly around Hong Kong, is characterized by relatively low turbidity (Owen, 2005), whilst suspended sediment plumes tend to concentrate on the western side of the estuary and flow southwestwards when they reach offshore Macau.

Tidal range within the estuary averages 0.86 m at the mouth to 1.57 m at Humen, but increases to 2.29 m and 3.36 m, respectively, during astronomical tides (Huang *et al*., 2004). Despite the small tidal range, the average volume of flood tide is as high as 73 500 m^3/s, which is nearly 13 times the average freshwater discharge (Xu *et al*., 1985). Each year one or two typhoons strike the area (Chan and Shi, 2000) and can generate storm surges of 1.40 to 1.80 m high that move into the estuary (Huang *et al*., 1982). Wind-driven waves and currents have minimal impact on sediment transport within the estuary in comparison with tidal currents (Owen, 2005). Protected from storm waves by the offshore rocky islands, wave energy within the estuary is low, except during the passage of a typhoon. During typhoons wave heights in excess of 1.5 m are common.

Methods

Surface sediment collection and analysis

Surface sediment samples were obtained from 77 locations (Figure 1B), for analyses of particle size distribution and diatom assemblages. These samples were collected from a variety of water depths from distributary channels of the delta plains, the estuary and the non-deltaic marine environment southeast offshore from Hong Kong (Figure 1B). At each sampling site, the top 10 cm of sediment were obtained using a grab sampler. Water depth and salinity were measured in both winter and summer seasons. Particle size analysis was carried out through a laser granulometer (Coulter LS 13200) to obtain the sand, silt and clay fractions. The technical procedure for diatom analysis followed those described by Palmer and Abbott (1986). A minimum count of 300 diatom valves was reached for all samples, and all diatoms were identified to a minimum of species level (eg, van der Werff and Huls, 1958–1966; Jin *et al*., 1982). They were then grouped into three categories (marine water, brackish water and fresh water) according to their salinity preferences (eg, Denys, 1991–1992). This modern data set (Table 2) was later used to characterize Holocene sedimentary types of the deltaic and estuarine systems.

Analysis of sediment cores

Seven sediment cores were drilled (PK16, M184, JT81, D13, NL, UV1 and V37; see locations in Figure 1B and details in Table 3) from the delta plain and estuary for detailed sedimentary and microfossil analyses. The core samples were obtained using push cores for soft, fine sediments, and rotary coring for stiff or more

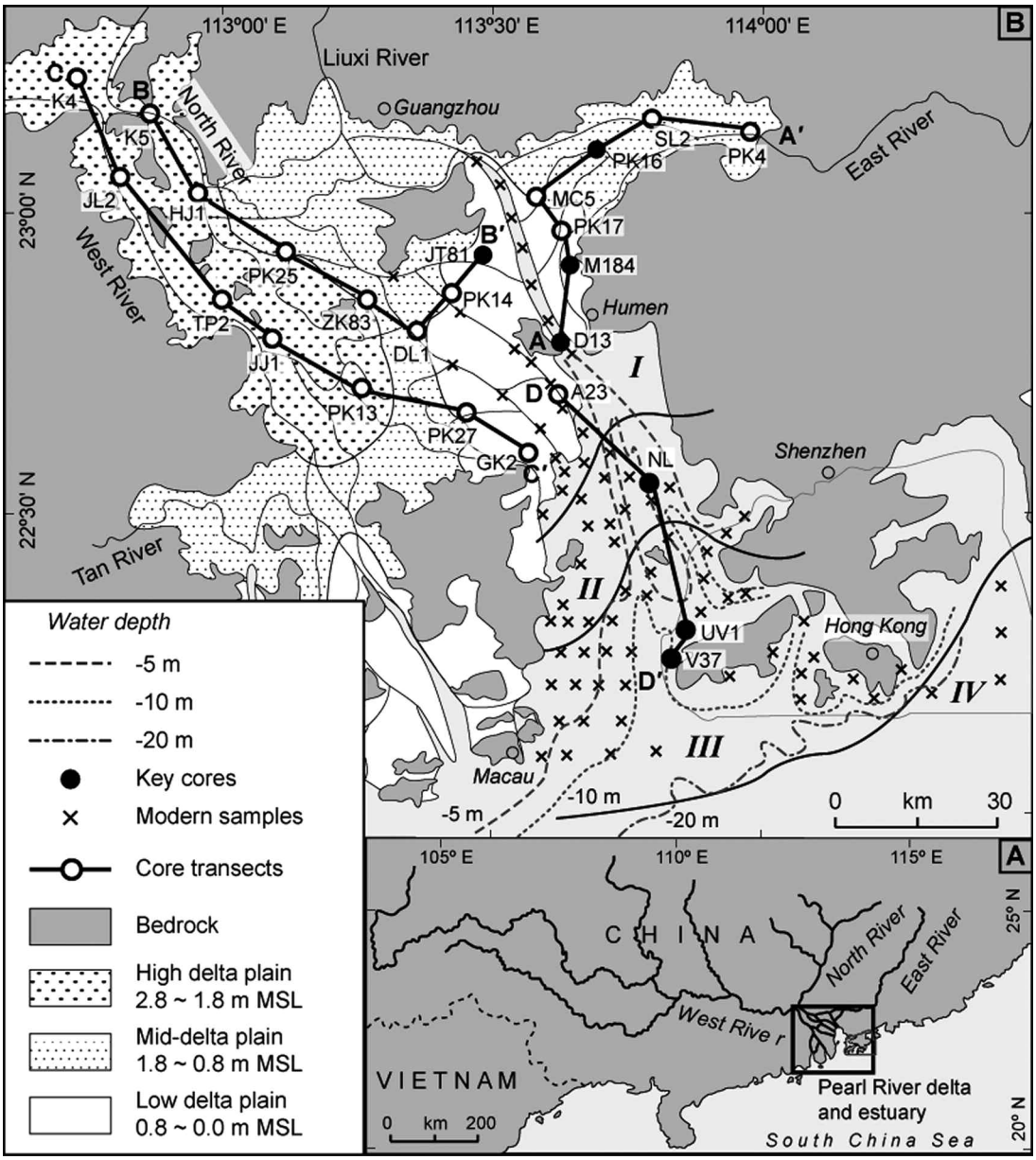

Figure 1 (A) The Pearl River catchment, with 79.8% of it being drained by the West River. (B) The Pearl River deltaic complex comprises the East River delta plain, the North and West Rivers delta plain, the estuary and the Tan River estuarine plain in the southwest. There are over 160 rocky islands of various sizes scattered within the deltaic plains and the estuary. Water depths of 5, 10 and 20 m are shown. Based on ground altitude and age of the emergence, the delta plains are divided into high, middle and lower parts. Locations of modern sediment samples (crosses), sediment cores (circles) and cross-section lines are shown. The seven key boreholes (filled circles) are named. The delta plains and estuary are divided into four deltaic facies zones: I, delta plain; II, delta front; III, pro-delta; IV, marine, according to Fyfe *et al*. (1997)

resistant coarse sediments. Another 18 representative core records were chosen from literature to complement the study as these core records provide sedimentary, microfossil and macrofossil information, and radiocarbon dates (Huang *et al*., 1982, 1985; Li *et al*., 1990). The core records provided information for the construction of a series of cross-sections across the deltaic plains and the estuary. Supplementary information was provided by another 279 core records from the deltaic plains, drilled for geological survey in the 1980s and 1990s. Based on information from these core records, a model for the early-Holocene palaeolandform evolution is reconstructed. A total of 34 radiocarbon dates, 16 of which are newly reported in this study, were obtained from plant fragments, bulk organic materials, oyster and marine shells and foraminifera samples (Table 4). Calibrated ages were calculated according to CALIB5.10 using the IntCal04 programme for terrestrial materials and the marine04 programme (Stuiver *et al*., 1998) for marine samples with a correction factor ΔR −128 ± 40 years according to Southon *et al*. (2002). A central calibrated age is given for each date and reported to nearest decade. Dates from bulk organic materials may be less reliable than other dates (Colman *et al*., 2002) because of potential inclusion of particulate organic carbon discharged from river systems (Raymond and Bauer, 2001).

Archaeological, historical and map data

Archaeological evidence, such as shell mounds and historical records on village development and land reclamation on the delta plain, were reviewed based primarily on the work of Li *et al*. (1990). Based on the spatial distribution of shell mounds, villages of different dynasties and records of land reclamation, several former shorelines were identified. Modern survey maps at 1:10 000 scale with ground altitude measured to 0.1 m were used to classify and characterize present-day landforms (Figure 1B).

Table 1 A comparison between the Pearl River delta and other Asian deltas

River	Length (km)	Catchment (km^2)	Water discharge (million m^3/yr) (% total)	Sediment discharge (million t/yr) (% total)	Average sediment content (kg/m^3)	Deltaic area (km^2)
West	2214	340 000	222 000 (73.5%)	72.5 (86.9%)	0.334	
North	573	46 500	41 000 (13.6%)	5.2 (6.2%)	0.126	
East	562	32 900	22 000 (7.3%)	3.1 (3.7%)	0.136	
Other small rivers		6 300	17 000 (5.6%)	2.6 (3.2%)	0.153	
Pearl River (total)[a]	**2214**	**425 700**	**302 000**	**83.4**	**0.276**	**9750**
Yangtze[b]	6380	1 807 000	953 500	478.0	0.510	52 000
Song Hong River[c]	1200	160 000	120 000	130.0	1.083	10 300
Mekong[d]	4620	810 000	470 000	160.0	0.340	93 781

[a] Huang *et al.* (1982) (according to data from 1952 to 1980); [b] Saito *et al.* (2001); [c] Tanabe *et al.* (2006); [d]Ta *et al.* (2002).
NB: Zhang *et al.* (2008) reported that the average sediment discharge from the Pearl River has declined to 54.0 million t/a yr for the period of 1996–2004 because of the construction of reservoirs in the catchment area. The deltaic area includes the deltaic plains of 5650 km^2, the estuary 1740 km^2 and rocky islands of 2360 km^2.

Table 2 Present-day sedimentary and environmental characteristics of the Pearl River delta

Sedimentary facies		Particle size (%)			Diatoms (%)			Water salinity (‰)		Water depth (m)
		Sand	Silt	Clay	Marine	Brackish	Freshwater	Summer	Winter	
Delta plain	tidal flat (channel and sandy shoal)	16.2 ± 7.3 (41.1 ± 12.0)	59.4 ± 6.7 (45.1 ± 8.3)	24.5 ± 5.9 (13.8 ± 5.3)	2.8 ± 2.6	15.1 ± 10.9	82.1 ± 13.1	2.1 ± 2.3	7.5 ± 5.5	3.9 ± 2.3
Delta front	subtidal flat (channel and sandy shoal)	12.8 ± 5.0 (32.2 ± 15.7)	58.1 ± 4.9 (46.6 ± 10.5)	29.1 ± 4.8 (21.2 ± 7.8)	13.2 ± 4.1	55.6 ± 10.2	31.2 ± 11.2	12.7 ± 4.3	21.2 ± 3.6	7.9 ± 5.0
Pro-delta	subtidal flat (channel)	14.9 ± 4.4 (26.0 ± 11.7)	57.8 ± 6.0 (52.2 ± 8.7)	27.3 ± 5.1 (21.8 ± 5.0)	43.1 ± 16.4	49.2 ± 13.8	7.7 ± 6.4	25.0 ± 6.0	30.0 ± 3.7	11.1 ± 6.4
Marine		13.7 ± 7.2	63.0 ± 5.4	23.2 ± 3.9	66.7 ± 2.1	33.1 ± 2.1	0.3 ± 0.3	33.8 ± 0.1	33.1 ± 0.2	27.0 ± 3.2

Results and interpretation

Sedimentary characteristics in the present-day environment

The particle size and diatom results from the 77 surface sediment samples are shown in Figure 2 and summarized in Table 2. These samples are grouped according to the delta plain, delta front, pro-delta environments and a non-deltaic marine environment, as defined by Fyfe *et al*. (1997) and adopted by Fyfe *et al*. (1999) and Owen (2005).

The results indicate that sand content is relatively high in tidal channels and sandy shoals of the delta plain environment (41.1 ± 12.0%) (Table 2), which is progressively lower from the delta front environment (32.2–15.7%) to the pro-delta environment (26.0 ± 11.7%). Tidal and subtidal flats in all environments are dominated by sandy mud and the sand content in most locations is comparatively low, around 15%. Silt and clay contents are both relatively consistent between the three deltaic environments. Diatom results indicate much clearer differences between the three deltaic environments. Within the delta plain environment, diatom assemblages are dominated by freshwater diatoms (over 80%, Figure 2) corresponding to low water salinity in both summer and winter seasons. The assemblages in the delta front environment are characterized by the high numbers of brackish water diatoms (55.6 ± 10.2%), together with variable amount of freshwater diatoms (31.2 ± 11.2%) and a minor percentage of marine diatoms (13.2 ± 4.1%). The diatom assemblages mirror closely the mid-range of water salinity (12.7 ± 4.3‰ in summer and 21.2 ± 3.6‰ in winter) suggesting they provide a reliable proxy for reconstructing palaeosalinities and environments. In the pro-delta environment, brackish water diatoms are still high (49.2 ± 13.8%). The marine diatoms though are highly variable, between about 20% and 60%. Four samples were collected from southeast of Hong Kong (Figure 1B), where summer water salinity is slightly higher than winter water salinity (Table 2), owing to strong evaporation in summer. Here the diatom assemblages are chiefly marine, whilst the sediments are mainly silt and clay.

The East River delta plain

In the East River delta plain a thick basal layer of sands and gravels (Figure 3) overlies bedrock along the incised valley floor. In core PK16, a freshwater peat sample at 15.9 m is dated to the late Pleistocene (Zong *et al*., 2009). Together with the slightly older dates from core PK4, this layer of sandy gravels is provisionally considered as deposits of the warm period of marine isotope stage (MIS) 3. Overlying this unit is a Holocene deltaic sequence up to 15 m thick. The deltaic sequence starts with a lower fine sand unit, from which a sample of plant fragment at 12.9 m in core PK16 is dated to 7010 cal. yr BP. The sequence grades vertically to a coarse sand unit, then a silt and clay unit. A bulk organic sample at 1.6 m of the silt-clay unit yields a date of 2840 cal. yr BP. The sediments between 12.9 m and 5.5 m contain dominantly brackish water diatoms with 10% to 20% of freshwater species (Figure 4). Comparison with the sedimentary characteristics of the present

Table 3 The lithological records of selected sediment cores

Depth (m)	Descriptions
Core PK16 (Alt. 0.8 m, mean sea level, N23°04′04″, E113°38′34″)	
0.0 – 0.5	Disturbed sandy sediments
0.5 – 5.5	Dark grey, soft, silt and clay with fine sands
5.5 – 7.5	Grey, coarse sands
7.5 – 12.9	Grey, soft, silt and fine sands
12.9 – 36.4	Yellowish grey, sands and gravels with thin organic layers
36.4 –	Bedrock (sandstone)
Core M184 (Alt. 0.1 m, mean sea level, N22°51′23″, E113°38′05″)	
0.0 – 1.6	Disturbed silt and clay
1.6 – 12.0	Dark grey silt and clay
12.0 – 16.9	Yellow coarse sands
16.9 –	Bedrock (granite)
Core JT81 (Alt. 0.5 m, mean sea level, N22°56′29″, E113°29′35″)	
0.0 – 1.2	Disturbed sandy sediments
1.2 – 14.1	Dark grey, soft, silt and clay
14.1 – 15.8	Yellowish grey, fine sands
15.8 – 18.0	Grey, soft, silt and clay (older marine sequence)
18.0 – 21.3	Yellow, coarse sands and gravels
21.3 –	Bedrock (sandstone)
Core D13 (Alt. −5.5 m, mean sea level, N22°47′19″, E113°35′57″)	
0.0 – 6.4	Dark grey, soft, silt and clay
6.4 – 14.2	Grey, soft to firm, fine sands with silt and clay
14.2 – 16.5	Grey, coarse sands with clay
16.5 – 27.3	Yellow, coarse sands and gravels
27.3 –	Bedrock (granite)
Core NL (Alt. −4.9 m, mean sea level, N22°27’50″, E113°46’13″)	
0.0 – 11.2	Dark grey, soft, silt and clay
11.2 – 12.0	Yellowish and reddish, firm, silt and clay
12.0 –	Grey, soft to firm, silt and clay (older marine sequence)
Core UV1 (Alt. −9.0 m, mean sea level, N22°17′10″, E113°51′49″)	
0.0 – 10.2	Dark greenish grey, soft, silt and clay
10.2 – 10.6	Bluish grey, firm, silt and clay with small gravels and coarse sands
10.6 –	Bluish, soft, silt and clay (older marine sequence)
Core V37 (Alt. −1.5 m, mean sea level, N22°15′02″, E113°51′29″)	
0.0 – 2.0	Dark greenish grey, slightly sandy clayey silt
2.0 – 10.1	Soft, dark greenish grey, clayey silt
10.1 – 10.6	Firm, dark grey, clayey silt with fine gravels
10.6 – 13.4	Light yellowish brown and spotted red silt and clay

environments (Table 2) suggests that the fine and coarse sands are most likely tidal channel deposits under delta front environment. Overlying this is a soft silt and clay layer where freshwater diatoms increase from 20% at 5 m to over 60% at 2 m, indicating a change from delta front environment to delta plain environment and a regressive process before 3000 cal. yr BP.

The sedimentary history recorded in core PK16 is mirrored in cores SL2 and PK4 (Figure 3). Extending towards the estuary, the middle-Holocene sandy units in core PK16 change into a thin layer of fine sands overlain by silt and clay in cores MC5, PK17, M184 and D13 (Figure 3). Brackish water diatoms dominate the sediment sequences throughout core M184 (Figure 4), with the exception of the lowest 8 m where marine diatoms increase to approximately 15% or higher, suggesting a delta front environment. Supporting the interpretation of a regressive delta is the replacement of the small marine diatom fraction with freshwater diatoms toward the top of the core. Freshwater diatoms reach 20% at 2.5 m where a bulk organic sample is dated to 1680 cal. yr BP (Table 4), indicating a change from delta front to delta plain after 1600 cal. yr BP. In core D13, the diatom assemblages are dominated by brackish water species, with about 20% of marine taxa, suggesting a stronger marine influence.

The North and West Rivers delta plain

In the North and West river valleys the basal unit is late-Pleistocene sandy gravel or weathered clay, overlain by a Holocene deltaic sequence (Figure 3). In the North River cross-section (B–B′, Figure 3), initial deltaic sedimentation is recorded by a thin layer of fine sands, observed in cores PK25 and JT81, and dated to 8620 and 8250 cal. yr BP, respectively. Particle size analysis of the fine sands from core PK25 suggests strong fluvial influence (Huang and Zong, 1982). The lower fine-sand layer in core JT81 contains dominant freshwater diatom assemblages with about 15% marine and brackish diatoms (Figure 4), thus the fine sands are considered as tidal channel deposits of delta plain environment. Overlying this fine-sand layer is silt and clay which contains abundant brackish water diatoms, for example in cores PK25 and ZK83 (Li *et al*., 1990). In core JT81 (Figure 4), the dominance of brackish water diatoms from the silt and clay sequence indicate a delta front environment.

In core DL1, a layer of fine sands appears at the middle of the deltaic silt-clay sequence. A fine sand layer is also recorded at a similar altitude in core PK14, which is dated to 5800 cal. yr BP. The abundance of brackish water diatoms from the silt-clay sequence of the similar altitude in cores PK25, ZK83 and JT81 suggests that this middle fine-sand layer is likely delta front tidal channel deposits.

Between core K5 and core DL1, a layer of fine sands is recorded overlying the silt-clay sequence. The particle size of these fine-sand layers suggests a fluvial origin (Huang and Zong, 1982). This upper fine-sand layer may represent the emergence of the delta plain. In core JT81, the increase in freshwater diatoms towards the top of the core (Figure 4) suggests a change from delta front environment to delta plain environment, which took place soon after 1260 cal. yr BP.

Along the West River cross-section (C–C′, Figure 3), Holocene deltaic sedimentation started with or without the lower layer of fine sands, followed by a sequence of silt and clay which contains abundant brackish water diatoms in cores JJ1 and GK2 (Li *et al*., 1990), as well as oyster shells in cores JL2, PK13 and PK27 (Huang *et al*., 1982), suggesting a delta front environment. On top of the fine delta front sequence is an upper layer of fine sand, which extends from core K4 to core GK2 and represents the emergence of the delta plain starting shortly after 4370 cal. yr BP at core JL2. The upper sand layer here is much thicker than that in the North River and East River delta plains, because of the much higher runoff and sediment supply from the West River (Table 1).

The estuary

Within the estuary, the Holocene deltaic sequence is much simpler (cross-section D–D′, Figure 3). Cores A23, NL, UV1 and V37 show mostly uniform silt and clay overlying weathered clay or sandy gravel. The foraminiferal assemblages in core NL (Huang, 2000) indicate a change from pro-delta environment at the base of the sequence before 7080 cal. yr BP to delta front environment in the rest of the sequence. In cores UV1 and V37, brackish water diatoms dominate the assemblages (Figure 4). Marine diatoms are relatively low in abundance in the lower part of core UV1 and the postglacial sedimentation started around 6190 cal. yr BP at this location. In the upper part of the core, marine diatoms increase to and exceed 20%, indicating a pro-delta environment. This change took place at *c*. 5000 cal. yr BP. According to the percentages of marine and brackish water diatoms, the environmental conditions in core V37 change from a pro-delta environment in the lower part of the core to a delta front environment in the middle part of the core shortly before 7620 cal. yr BP, and then back to pro-delta environment in the upper part of the core around 5000 cal. yr BP (Figure 5).

Table 4 Age determination for the sedimentary sequences of the Pearl River delta

Sediment type and facies	Core	Depth (m)	Material dated	Method	Conventional age (yr BP)	Calibrated age (yr BP) (1σ)	Central cal. age (yr BP)[a]	Laboratory code	Ref.[b]
The East River delta plain cross-section									
Delta front (oyster shells)	PK17	3.5	Bulk organic	Conv. ^{14}C	1520 ± 90	1613–1289	1450	KWG-13	B
Delta front (brackish water diatoms)	M184	2.5	Bulk organic	Conv. ^{14}C	1740 ± 75	1835–1520	1680	KWG-1001	C
Delta front (brackish water diatoms)	PK16	1.6	Bulk organic	Conv. ^{14}C	2670 ± 85	3000–2685	2840	KWG-100	B
Delta front (brackish water diatoms)	D13	6.7	Bulk organic	Conv. ^{14}C	4210 ± 100	4982–4513	4750	KWG-744	A
Delta front (brackish water diatoms)	PK16	12.9	Plant fragment	Conv. ^{14}C	6150 ± 160	7340–6677	7010	GC-520	B
Delta front (oyster shells)	PK4	4.7	Plant fragment	Conv. ^{14}C	5940 ± 300	7441–6185	6810	KWG-5	B
Delta front (brackish water diatoms)	M184	7.8	Bulk organic	Conv. ^{14}C	7200 ± 130	8172–7931	8050	KWG-840	C
The North River delta plain cross-section									
Delta front (brackish water diatoms)	JT81	3.9	Bulk organic	Conv. ^{14}C	1310 ± 65	1299–1225	1260	KWG-693	A
Delta front (oyster shells)	PK14	6.7	Oyster shell	Conv. ^{14}C	1680 ± 90	1618–1544	1580	KWG-43	B
Delta front (brackish water diatoms)	JT81	5.9	Bulk organic	Conv. ^{14}C	2430 ± 90	2519–2359	2440	KWG-690	A
Delta front (brackish water diatoms)	JT81	10.7	Bulk organic	Conv. ^{14}C	3840 ± 95	4416–4154	4290	KWG-700	A
Delta front (oyster shells)	PK14	9.7	Bulk organic	Conv. ^{14}C	5020 ± 160	6135–5470	5800	KWG-46	B
Delta plain (freshwater diatoms)	K5	7.0	Plant fragment	Conv. ^{14}C	6300 ± 300	7713–6483	7100	KWG-8	B
Delta front (brackish water diatoms)	ZK83	13.0	Oyster shell	Conv. ^{14}C	6620 ± 170	7663–7415	7540	KWG-77	C
Fluvial sand	JT81	14.9	Plant fragment	Conv. ^{14}C	7390 ± 140	8351–8157	8250	KWG-890	A
Fluvial sand	PK25	12.6	Plant fragment	Conv. ^{14}C	7830 ± 220	8809–8429	8620	KWG-423	C
The West River delta plain cross-section									
Delta front (oyster shells)	JL2	8.1	Oyster shell	Conv. ^{14}C	3950 ± 150	4583–4154	4370	GC-687	C
Delta front (oyster shells)	GK2	9.9	Bulk organic	Conv. ^{14}C	4710 ± 120	5493–5320	5410	KWG-99	C
Delta front (brackish water diatoms)	JJ1	9.4	Bulk organic	Conv. ^{14}C	4820 ± 120	5661–5449	5560	KWG-902	C
Delta front (oyster shells)	PK13	9.7	Oyster shell	Conv. ^{14}C	4940 ± 250	5941–5447	5690	GC-483	C
Delta front (oyster shells)	PK27	9.0	Oyster shell	Conv. ^{14}C	5790 ± 170	6981–6281	6630	KWG-40	B
Fluvial sand	JJ1	18.4	Freshwater shell	Conv. ^{14}C	8380 ± 140	9529–9252	9390	KWG-901	C
The Estuary cross-section									
Delta front (brackish water diatoms)	A23	4.3	Bulk organic	Conv. ^{14}C	1610 ± 80	1700–1351	1530	KWG-62	B
Pro-delta (marine/brackish water diatoms)	UV1	1.9	Foraminifera	AMS ^{14}C	3019 ± 35	3009–2851	2930	SUERC9602	A
Delta front (estuarine foraminifera)	NL	3.6	Foraminifera	Conv. ^{14}C	3340 ± 110	3490–3200	3350	KWG-H9610	A
Pro-delta (marine/brackish water diatoms)	V37	2.0	Foraminifera	AMS ^{14}C	3470 ± 40	3564–3420	3490	Beta193746	A
Pro-delta (marine/brackish water diatoms)	UV1	4.5	Foraminifera	AMS ^{14}C	3963 ± 35	4229–4060	4150	SUERC9605	A
Pro-delta (marine/brackish water diatoms)	V37	2.9	Foraminifera	AMS ^{14}C	4330 ± 40	4725–4555	4640	Beta193747	A
Delta front (brackish water diatoms)	UV1	7.5	Foraminifera	AMS ^{14}C	4847 ± 35	5412–5274	5340	SUERC9606	A
Delta front (estuarine foraminifera)	NL	7.4	Foraminifera	Conv. ^{14}C	5540 ± 120	6202–5929	6070	KWG-H9612	A
Delta front (brackish water diatoms)	UV1	9.5	Foraminifera	AMS ^{14}C	5633 ± 36	6259–6129	6190	SUERC9607	A
Pro-delta (marine foraminifera)	NL	10.1	Foraminifera	Conv. ^{14}C	6450 ± 200	7302–6856	7080	KWG-H9610	A
Delta front (brackish water diatoms)	V37	7.0	Foraminifera	AMS ^{14}C	7020 ± 40	7666–7565	7620	Beta193748	A
Pro-delta (marine/brackish water diatoms)	V37	9.7	Foraminifera	AMS ^{14}C	7970 ± 40	8631–8474	8550	Beta193749	A

[a] Central calibrated ages are reported to nearest decade. [b] References: A, this study, B, Huang *et al.* (1982); C, Li *et al*. (1990).

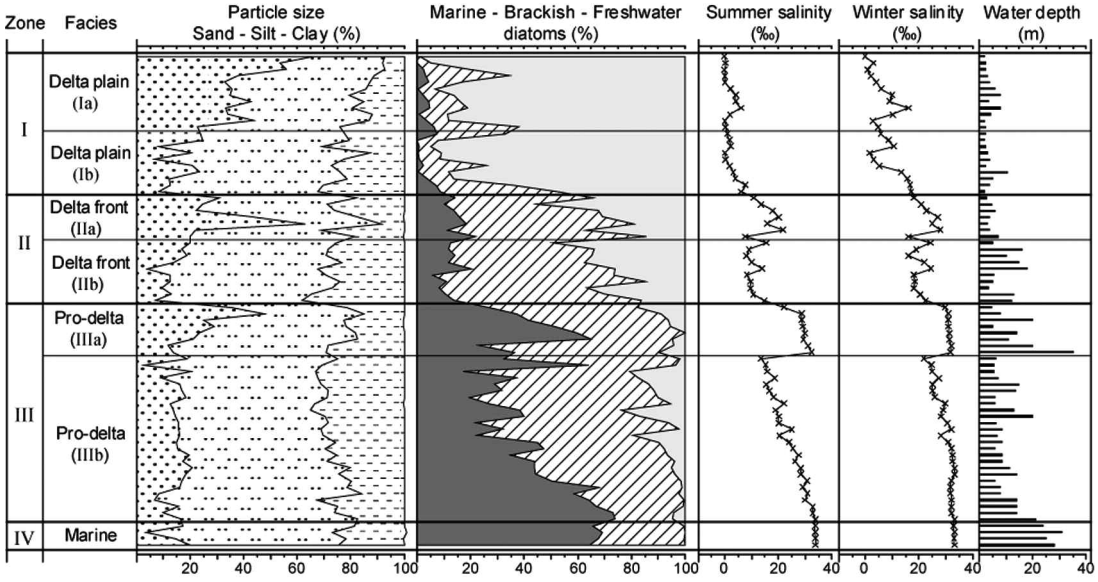

Figure 2 Particle size, diatom assemblages, water salinity and water depth of each modern sediment sample. Samples are grouped into the delta plain (Ia, distributary channel and sandy shoal; Ib, tidal flat), delta front (IIa, subtidal channel and sandy shoal; IIb, subtidal flat), pro-delta (IIIa, subtidal channel; IIIb, subtidal flat) and marine zones (see summary in Table 2)

Palaeo-shorelines

The position of the most landward shoreline (*c*. 6800 cal. yr BP) is identified based on a large number of Neolithic shell mounds found around the apex of the deltaic plains (Figure 5). On the inland side of this shoreline, shell mounds contain mainly freshwater species, yet on the seaward side most of shells are of brackish water origin. The oldest three shell mounds were dated to between 6670 and 7010 cal. yr BP (Li *et al*., 1990). This shoreline is supported by sedimentary evidence (Figure 3). Brackish water diatoms are found from the deltaic sequence of core PK4 (4.1 m, after 6810 cal. yr BP) near the apex of the East River delta plain and core K5 (6.8 m, after 7090 cal. yr BP) near the apex of the North and West River delta plain (Figure 3). The second shoreline (*c*. 4500 cal. yr BP) marks the seaward limit of the Neolithic shell mounds, and the youngest mound was dated to 4340 cal. yr BP (Li *et al*., 1990). Soon after *c*. 4000 cal. yr BP, the Neolithic communities in the area changed from hunting-gathering to farming (Zheng *et al*., 2003). However, comprehensive sedimentary evidence for this shoreline has yet to be identified.

Around the beginning of the Han Dynasty (206 BC to AD 220), population in the area increased and agricultural cultivation intensified. Many villages were established on the emerged delta plain. Li *et al*. (1990) defined the 2000 yr BP shoreline based on the seaward limit of Han villages and tombs. On the same basis, the 1000 yr BP shoreline is identified as running through a line of villages and tombs of the Song Dynasty (AD 960–1279). This shoreline separates villages and tombs of the Tang Dynasty (AD 618–907) found on the landward side from villages and tombs of the Ming Dynasty (AD 1368–1644) found on the seaward side of the shoreline (Li *et al*., 1990). The 2000 yr BP shoreline in the East River delta plain is supported by sedimentary evidence that a change from delta front environment to delta plain environment took place soon after 2840 cal. yr BP in core PK16 (Figure 4). Similarly, the 1000 yr BP shoreline in the North River delta plain is supported by the change in diatoms from delta front to delta plain soon after 1260 cal. yr BP in core JT81 (Figure 4).

Discussion

Sea-level rise and marine transgression

The sedimentary record indicates that at the start of the Holocene deltaic sedimentation, the receiving basin was filled with an older (possibly OIS Stage 5e) estuarine unit and fluvial sands and gravels, with bedrock exposed in parts of the basin (Figure 6A). The depth of the receiving basin varies between 5 m near the apexes and 15–20 m in the depocentre. In the mouth area of the basin, the valleys incise to 25–30 m. Comparatively, the palaeobasin is much shallower and more complex than those in the Yangtze (60–100 m, Li *et al*., 2000), the Mekong (*c*. 70 m, Ta *et al*., 2002) and the Song Hong River (*c*. 40 m, Tanabe *et al*., 2006). The shallow nature of the receiving basin has resulted in being initially inundated by the sea as late as 9000 cal. yr BP when relative sea level rose to −20 m (Zong, 2004).

Based on the core records (Figures 3 and 4), the initial sedimentation took place along palaeoriver channels. This phase of sedimentation, such as the lower fine-sand layer in cores MC5, PK25, JT81, JJ1 and PK13, is recorded between −19 m and −12 m in altitude and dated to around 9500–8200 cal. yr BP. The deposition of this layer of fine sands is supported by strong monsoon-driven freshwater discharge (Wang *et al*., 2005). Soon after this phase of sedimentation, the deeper part of the receiving basin, ie, the area around cores GK2, PK13, JJ1, DL1 and D13 (Figure 3) was inundated by the sea, as a result of a rise in relative sea level from −20 m to −12 m (Zong, 2004). Areas around cores PK27 and A23 appeared to be locally higher ground. Around 8200 cal. yr BP, the inner part of the receiving basin was under fluvial influence, whilst the seawards part of the basin was under open estuarine conditions. A transitional zone was located approximately between cores JL2, ZK83, JT81, MC5 on the fluvial side and JJ1, PK13, DL1, D13 on the marine side (Figure 6B). This initial phase was followed by a period of widespread marine inundation in the receiving basin, as a result of two sharp rises in relative sea level from −12 m to −3 m (Zong, 2004) during 8200–8000 and 7500–7000 cal. yr BP (Yim *et al*., 2006; Bird *et al*., 2007). The rising sea level has

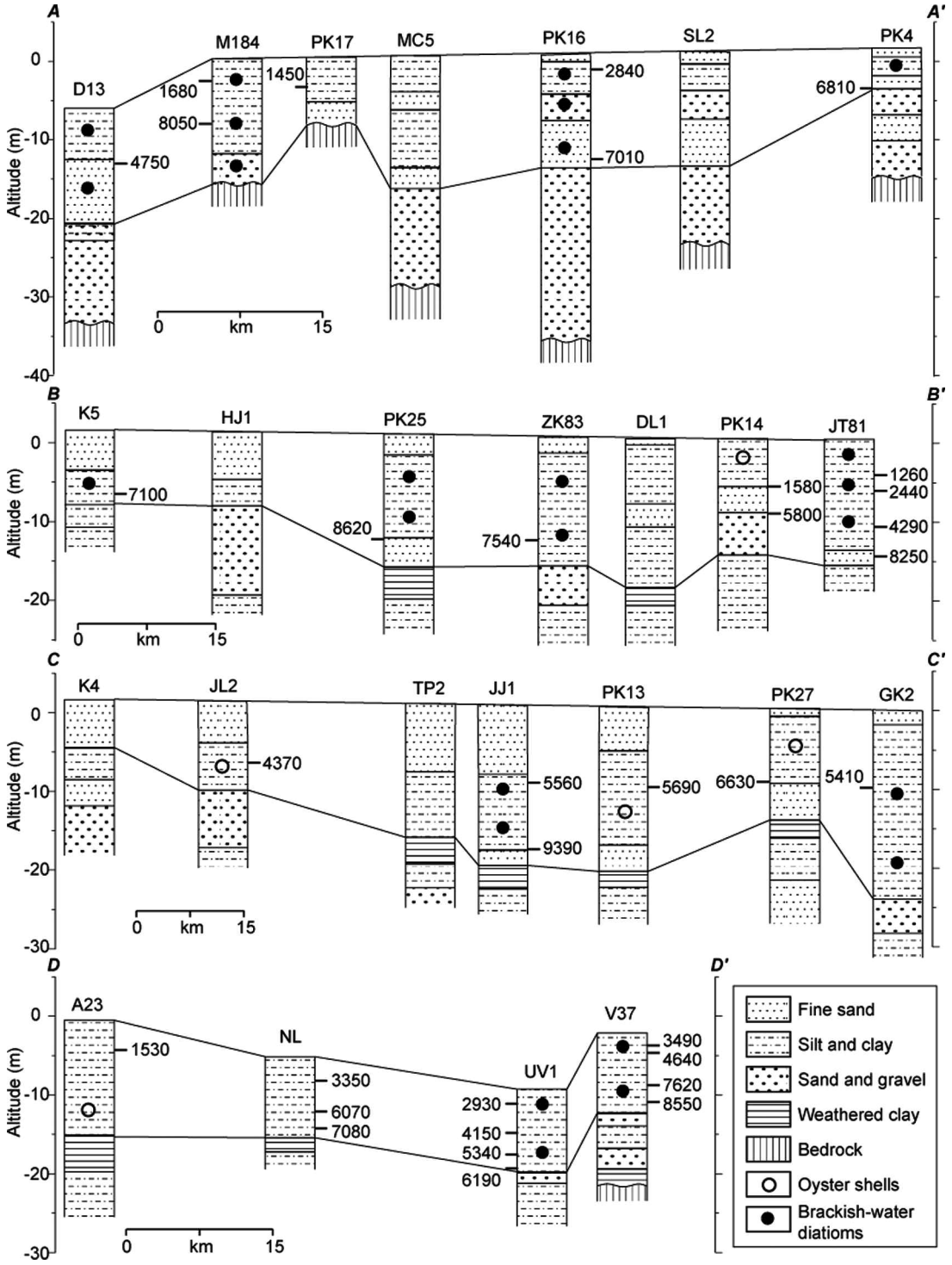

Figure 3 The cross-sections for the Pearl River delta complex. The radiocarbon dates are in calibrated years BP, and the central calibrated ages are reported to nearest decade (see details in Table 4). The connecting lines between sediment cores highlight the Holocene deltaic sequence

resulted in the sea advancing for about 75 km from core DL1 to the apex of the North and West Rivers delta plain. The deltaic shoreline was also pushed as far back as the apex of the East River delta plain. This widespread marine transgression in the receiving basin changed the sedimentary environments of the basin significantly with a switch from tidal sandy sedimentation along delta plain channels to deltaic silt and clay deposition. It is noted that in the area around cores NL and UV1, no sedimentation took place during this transgression period. In core V37, sedimentation started earlier, and possibly the sediments were from local sources.

Monsoonal water/sediment discharge and delta progradation

The first deltaic shoreline was developed near the apex of the delta plains (Figure 6C) at about 6800 cal. yr BP when relative sea level reached its present-day height and stabilized (Zong, 2004). Consequently the transgressive process changed to a regressive process, ie, the onset of deltaic progradation. Around 6800 cal. yr BP, most of the receiving basin was under delta front conditions, including the area around core NL (Figure 6C), where the foraminifera assemblages are dominated by estuarine species. This is due to monsoon-driven freshwater discharge that was

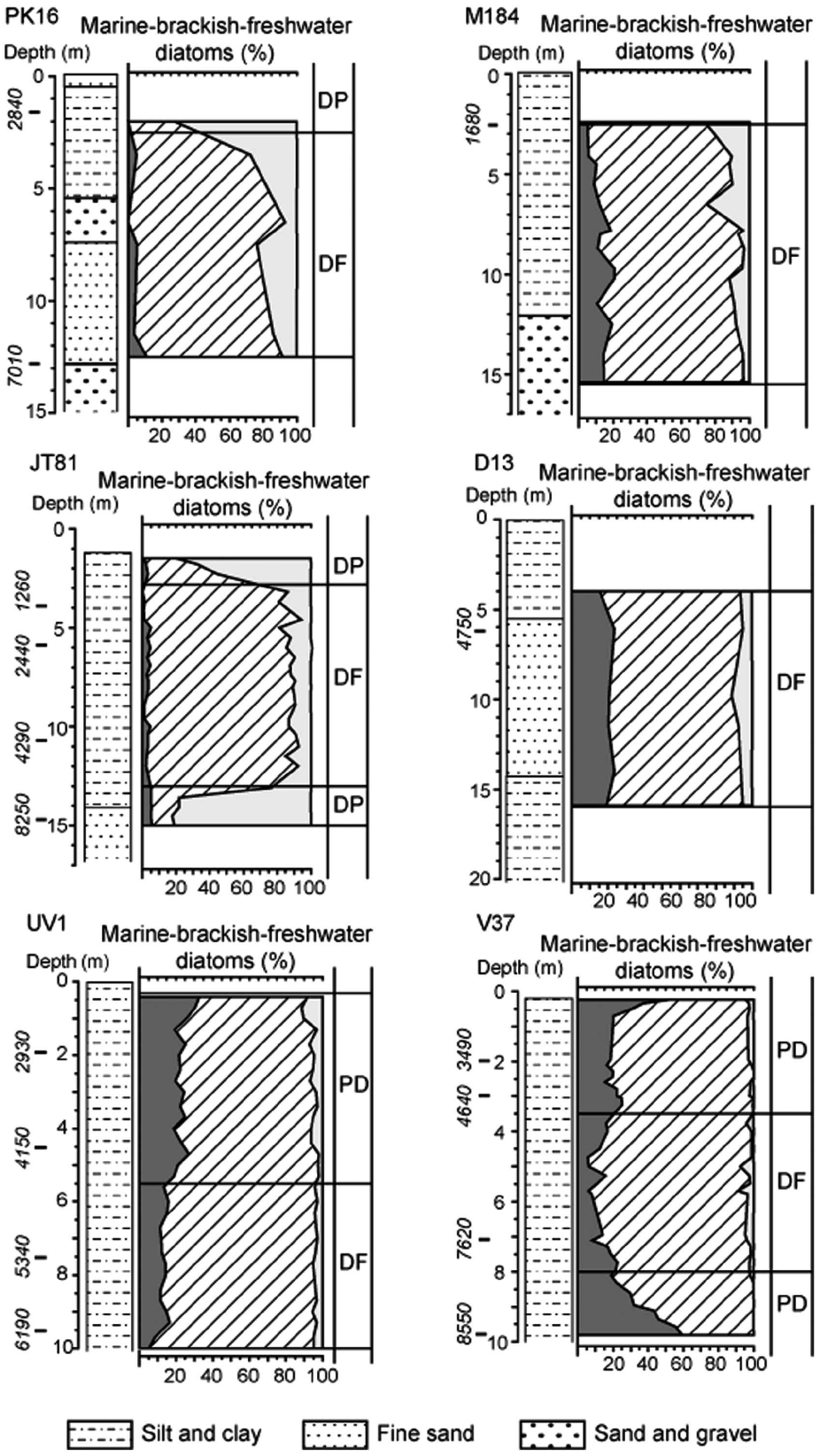

Figure 4 Sedimentary characteristics (see Table 3) and diatom results for cores PK16, M184, JT81, D13, UV1 and V37. The radiocarbon dates are in calibrated years BP (see details in Table 4). DP, delta plain; DF, delta front; PD, pro-delta

exceptionally high around this time (Zong *et al.*, 2006). Between 6800 and 2000 cal. yr BP, the deltaic shoreline advanced slowly seawards (Figure 5). By 2000 cal. yr BP (Figure 6D) about half of the deltaic plain had emerged. The shoreline is identified as being between cores PK16 and M184 because shortly before this time, core PK16 was already under delta plain conditions, whilst core M184 was still under delta front conditions for another 1000 years (Figure 3). Along the North and West Rivers, delta plain conditions (fluvial sandy sediments) spread as far as cores ZK83 and PK13 (Figure 3), but cores PK14, JT81, A23 and NL were all

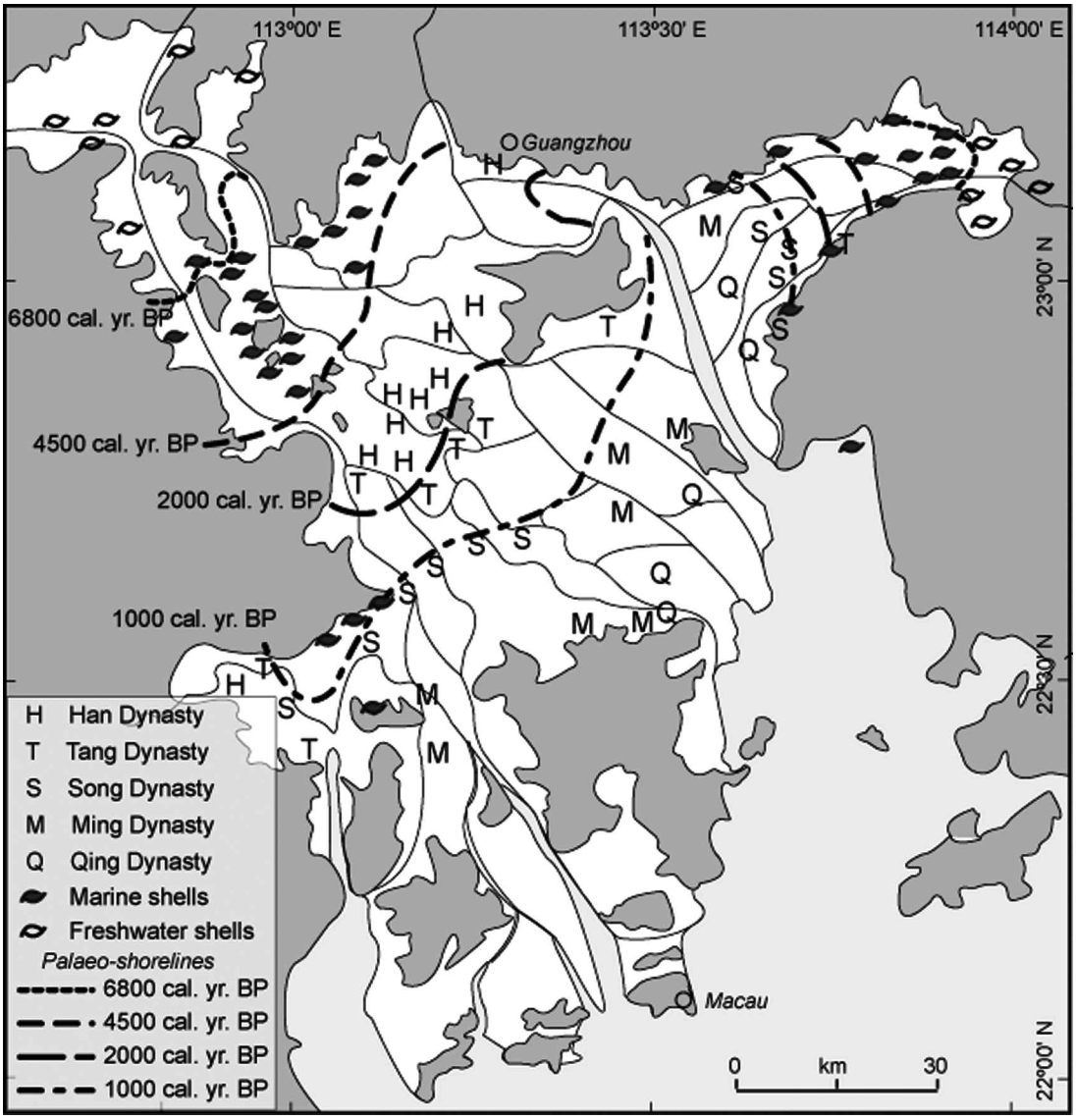

Figure 5 Palaeo-shorelines as estimated based on archaeological evidence and historical records (revised after Li *et al*., 1990). Shell mounds, dated to between 6800 and 5000 cal. yr BP, contain dominantly freshwater shells or dominantly brackish water shells (Li *et al*., 1990). Villages shown were established in Han Dynasty (206 BC–AD 220), Tang Dynasty (AD 618–907), Song Dynasty (AD 960–1279), Ming Dynasty (AD 1368–1644) and Qing Dynasty (AD 1644–1911)

under delta front conditions. Despite the shoreline advance, cores UV1 and V37 reverted back to pro-delta conditions around 4500–5000 cal. yr BP (Figure 4). This may reflect a reduction in monsoon-driven fluvial runoff (Zong *et al*., 2006). Between *c*. 6800 and 2000 yr BP, the deltaic shoreline (the seawards limit of delta plain) had advanced for about 30 km on the East River delta plain and 40 km on the North and West Rivers delta plain. The palaeo-shorelines suggest a deltaic progradation rate of 10.5 m/yr between 6800 and 4500 cal. yr BP and 6.4 m/yr between 4500 and 2000 cal. yr BP for the North and West Rivers. The slowing in progradation rate is possibly a result of a gradual reduction in sediment supply because of a weakening summer monsoon (Wang *et al*., 2005) and monsoon-driven water discharge (Zong *et al*., 2006).

Human activities and recent shoreline advances

Between 4000 and 3000 cal. yr ago, a change from hunting-gathering to wet rice farming took place in the Pearl River delta area (Zheng *et al*., 2003). By the time of the Han Dynasty (206 BC–AD 220), large parts of the emerged delta plain were available for cultivation. Throughout the past 2000 years, people have employed various techniques to reclaim newly emerging parts of delta plain for agriculture. Primitive sea walls are found in many localities where farmers place a line of gravels and stones along the low tide mark on a tidal flat, raising its height each year. As a result, more and more sediments were trapped behind the ridge of stones and the altitude of the tidal flat increased. Finally, as the land surface of the tidal flat rose to the height above mean tide level, reclamation of the tidal flat was completed by building an earth bank or sea wall on the stone ridge.

These active land reclamation activities have two effects. First, shoreline advances were accelerated. In fact shoreline progradation in the past 2000 years has been up to 29 m/yr in the case of North and West Rivers (Figure 5), much faster than the rates of the previous 4800 years. Second, a large amount of sediment trapped along the edge of delta plains meant that the amount of sediments supplied to the estuary was reduced. This effect is demonstrated by the reduction in sedimentation rates recorded in cores NL, UV1 and V37 (Figure 7). Core JT81 shows a progressively increasing sedimentation rate towards present, from an average rate of 2.18

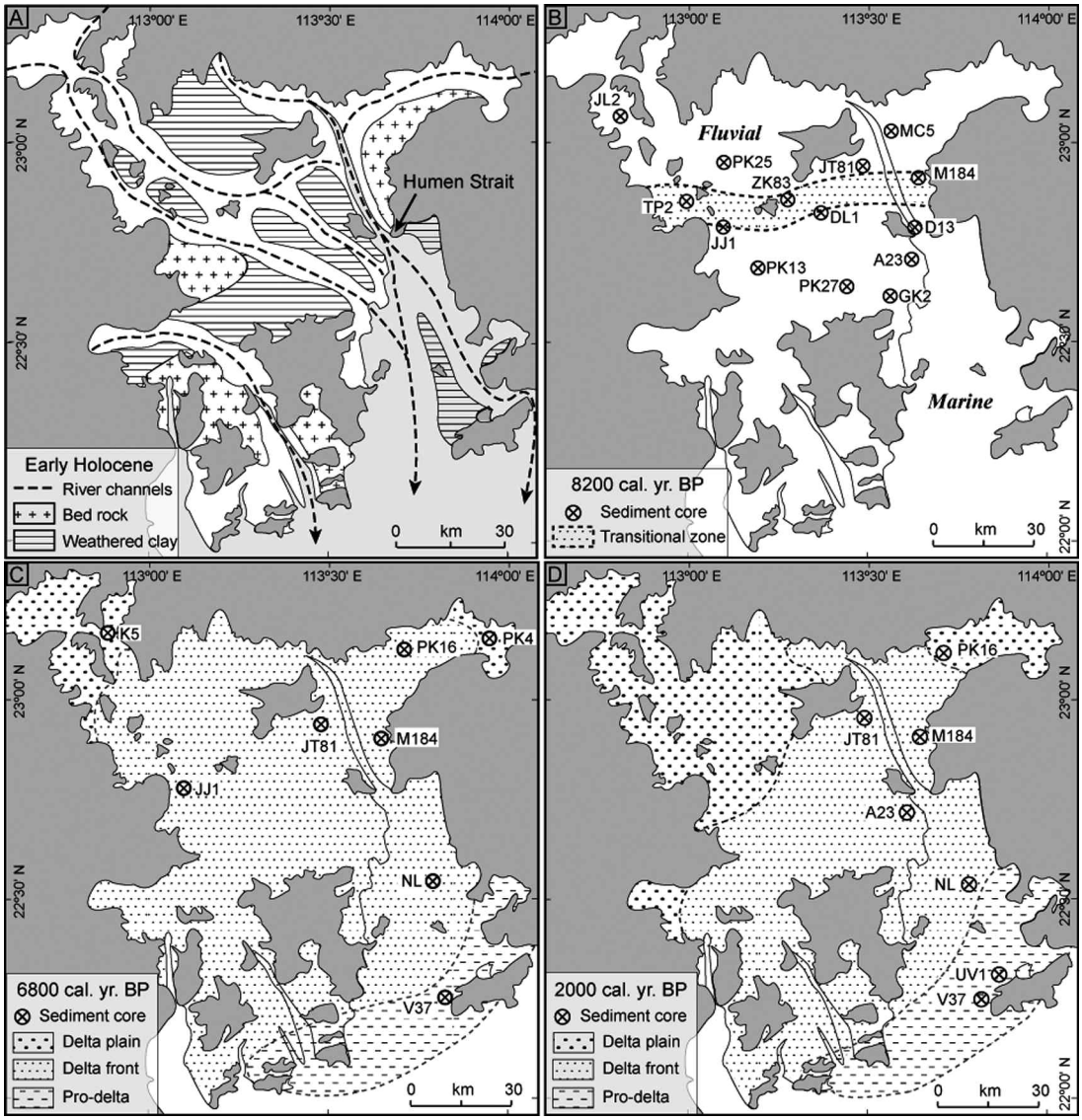

Figure 6 (A) The early-Holocene palaeo-landscapes of the receiving basin, with major palaeo-valleys filled with coarse sands and gravels, areas of bedrock exposed, and areas of older marine deposits capped by weathered clay or desiccated crust. (B) The marine limit before *c*. 8200 cal. yr BP, based on sedimentary evidence of the initial phase of sedimentation. (C) The deltaic sedimentary environments within the receiving basin when the rise in sea level stabilized and the shoreline retreated to its landward-most position around 6800 cal. yr BP. (D) The deltaic sedimentary environments within the receiving basin around 2000 cal. yr BP.

± 0.60 mm/yr between 4290 and 1260 cal. yr BP to 3.09 ± 0.10 mm/yr in the last 1200 years. Similarly high sedimentation rates (2.86 ± 0.33 mm/yr since 1530 cal. yr BP in core A23, and 4.24 ± 0.10 mm/yr since 1580 cal. yr BP in core PK14) are also recorded from the same area (Figure 3). However, the average sedimentation rate for the last 3000 years in cores NL, UV1 and V37 is only 0.77 ± 0.25 mm/yr, much lower than that of the previous 3000 years (1.76 ± 0.56 mm/yr). The reduction in sediment supply to the estuary may have coincided with the further reduction in monsoon-driven freshwater discharge (Zong *et al*., 2006).

A model of deltaic landform evolution

Based on all the evidence presented, we propose a three-stage conceptual model of Holocene landform evolution for the Pearl River delta (Figure 8).

Stage 1 (9000–6800 cal. yr BP)

During the early Holocene rapid sea-level rise was the dominant driving mechanism, with strong monsoon runoff as the secondary driving mechanism for a period of rapid environmental change. Under the combination of these two mechanisms, the receiving basin was inundated by the sea, and sedimentation changed from deltaic fine sands to deltaic silt and clay. Sedimentation took place mainly in the middle and upper parts of the basin. This stage saw a change from shallow tidal processes to deep tidal processes in the receiving basin. The transgressive processes in the Pearl River delta were initiated around 8000 years ago and switched to regressive processes 6800 years ago, as suggested by Stanley and Warne (1994).

Stage 2 (6800–2000 cal. yr BP)

As relative sea level stabilized and monsoonal discharge and tides became the dominant controlling variables for sedimentary processes, the delta started to grow. However, as summer monsoon started to weaken from 6000 cal. yr BP onwards, the progradation rate gradually reduced. As the delta plain prograded in the up-river areas, steady vertical aggradation of delta front sedimentation took place in the central and seaward parts of the receiving

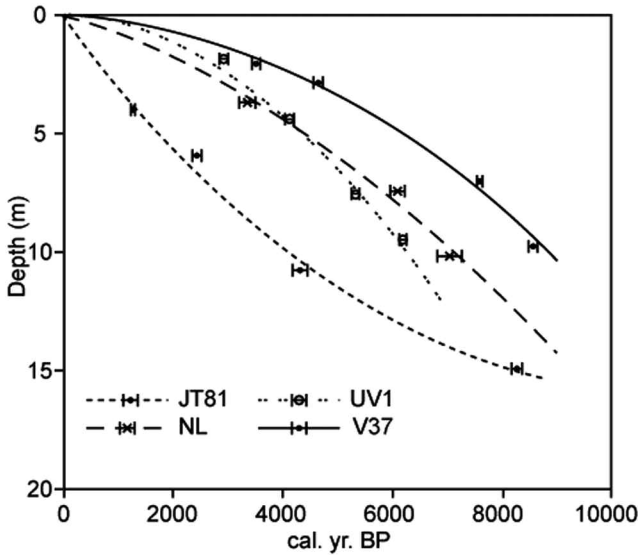

Figure 7 Changes in sedimentation rate recorded from cores JT81, NL, UV1 and V37

basin (Figure 8). The deltaic sedimentation was dominantly under delta front conditions, and sediments were modified by tidal processes, as suggested by Wu *et al*. (2007).

Stage 3 (2000 cal. yr BP to present)

This is a period of further weakening of monsoonal discharge, and an increase in human activities. Deforestation in the catchment increased soil erosion and sediment supply (Zhang *et al*., 2008). Some sediment may have been trapped in paddy fields on hillsides and small floodplains in the catchment area, but most was trapped in tidal flats and newly reclaimed delta plains, because of the particular practice of land reclamation, resulting in rapid shoreline advance. As a consequence, the amount of sediment draining into the estuary decreased, and hence the vertical accretion rate in the mouth area of the estuary was reduced.

This model is comparable with some other Asian deltas. Particularly the slower progradation rates at 6000–2000 cal. yr BP and the acceleration in shoreline advance in the last 2000 years are also recorded in the Yangtze (Hori *et al*., 2001), the Han River (Zong, 1989) and the Song Hong River (Tanabe *et al*., 2006), because they have also been under the influence of Asian monsoon climate and have a similar sea-level history. All these systems are affected by similar patterns of human activities, despite the differences in catchment size, water/sediment discharge and the size and shape of the receiving basins.

Conclusions

On the basis of a comprehensive survey and analysis of litho-biochronostratigraphy, we have reconstructed the Holocene evolutionary history of the Pearl River delta, and proposed a conceptual model and three driving factors for the three stages of delta formation. Sea-level change has been the major controlling factor determining the base level and available accommodation space for the delta to grow. Strong monsoonal runoff brought large amounts of sediment from the catchment to the receiving basin, where the sediments were reworked by tidal currents in the

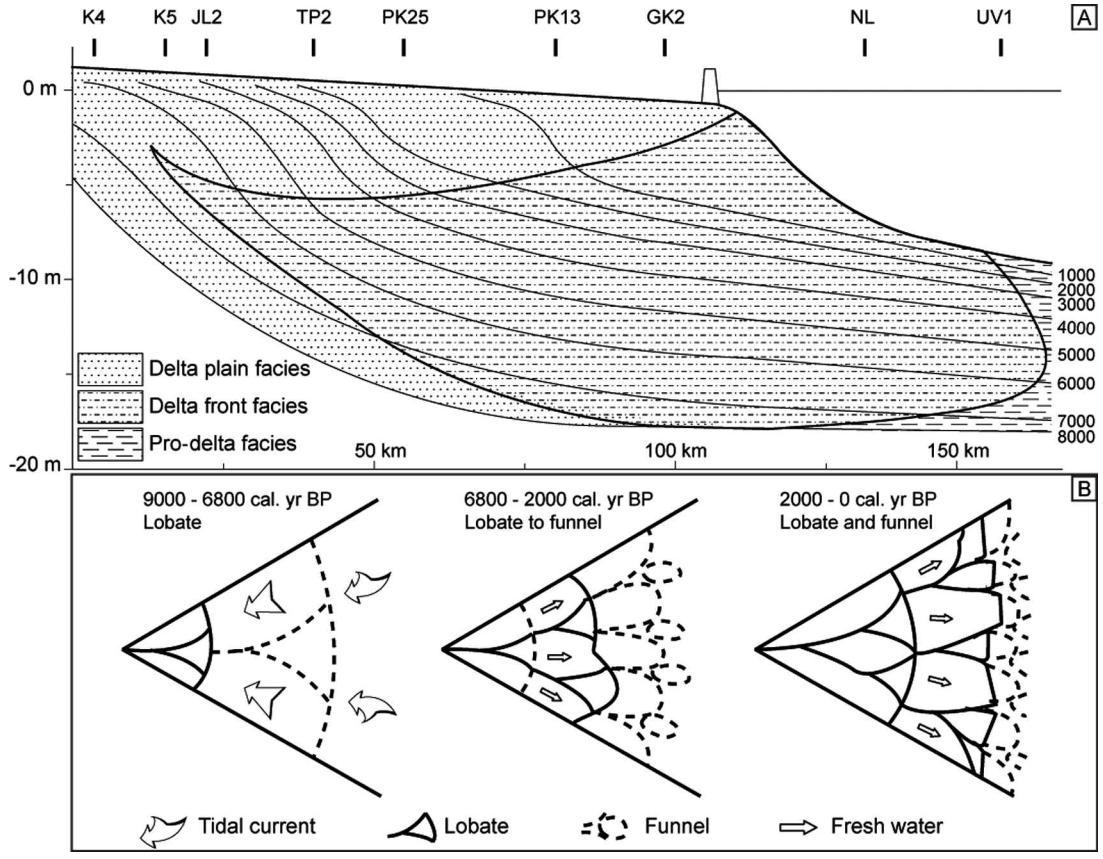

Figure 8 The development model for the Pearl River deltaic complex. (A) A schematic cross-section for the Pearl River deltaic complex, based on core records between the apexes of the North and West Rivers and the mouth of the estuary. (B) Dominant processes at different stages of deltaic development

initial stage of deltaic formation. As monsoonal discharge weakened progressively between 6800 and 2000 cal. yr BP, deltaic progradation slowed. In the last 2000 years, human activities intensified and land reclamation practices significantly altered the sedimentary processes. As large amount of sediments was trapped on encircled tidal flats, it accelerated the pace of delta shoreline advance and decreased estuary sediment accretion. This study demonstrates the importance of understanding key driving mechanisms of deltaic landform development and changes.

Acknowledgements

This research is supported by the University of Durham through a special research grant awarded to Zong, a grant from the Chinese National Science Foundation (Number 40771218) awarded to Huang and Zong, and a grant from the Research Grants Council of the Hong Kong Special Administration Region, China (Project No. HKU 7024/03P) awarded to Yim. Switzer is supported by a donation from the Business Environment Council of Hong Kong. The authors thank the director of the Environmental Protection Department, Hong Kong SAR Government, for the collection of surface sediment samples. This research is also supported by four radiocarbon dates awarded by the Natural Environment Research Council (UK) Radiocarbon Laboratory Steering Committee (Number 1150.1005). The authors would like to thank the two reviewers for their constructive comments which have helped improve the text.

References

Aitchison, J.C., Ali, J.R. and **Davies, A.M.** 2007: When and where did India and Asia collide? *Journal of Geophysical Research, Solid Earth* 112, B05423, doi: 10.1029/2006JB004706.

An, Z. 2000: The history and variability of the East Asian paleomonsoon climate. *Quaternary Science Reviews* 19, 171–87.

Bird, M.I., Fifield, L.K., The, T.S., Chang, C.H., Shirlaw, N. and **Lambeck, K.** 2007: An inflection in the rate of early mid-Holocene eustatic sea-level rise: a new sea-level curve from Singapore. *Estuarine, Coastal and Shelf Science* 71, 523–36.

Chan, J.C.L. and **Shi, J.** 2000: Frequency of typhoon landfall over Guangdong province of China during the period 1470–1931. *International Journal of Climatology* 20, 183–90.

Chen, Z., Watanabe, M. and **Wolanski, E.** 2007: Sedimentological and ecohydrological processes of Asian deltas: the Yangtze and the Mekong. *Estuarine, Coastal and Shelf Science* 71, 1–2.

Colman, S.M., Baucom, P.C., Bratton, J.F., Cronin, T.M., McGeehin, J.P., Willard, D., Zimmerman, A.R. and **Vogt, P.R.** 2002: Radiocarbon dating, chronology framework, and changes in accumulation rates of Holocene estuarine sediments from Chesapeake Bay. *Quaternary Research* 57, 58–70.

Denys, L. 1991–92: *A check list of the diatoms in the Holocene deposits of the western Belgian coastal plain with a survey of their apparent ecological requirements*. Professional Paper 246, Belgian Geological Survey.

Fyfe, J.A., Selby, I.C., Shaw, R., James, J.W.C. and **Evans, C.D.R.** 1997: Quaternary sea-level change on the continental shelf of Hong Kong. *Journal of the Geological Society, London* 154, 1031–38.

Fyfe, J.A., Selby, I.C., Plater, A.J. and **Wright, M.R.** 1999: Erosion and sedimentation associated with the last sea level rise offshore Hong Kong, South China Sea. *Quaternary International* 55, 93–100.

Goodbred, S.L., Jr and **Kuehl, S.A.** 2000: The significance of large sediment supply, active tectonism, and eustasy on margin sequence development: late Quaternary stratigraphy and evolution of the Ganges-Brahmaputra delta. *Sedimentary Geology* 133, 227–48.

Hori, K., Saito, Y., Zhao, Q., Cheng, X., Wang, P., Sato, Y. and **Li, C.** 2001: Sedimentary facies and Holocene progradation rates of the Changjiang (Yangtze) delta, China. *Geomorphology* 41, 233–48.

Huang, G. 2000: Holocene record of storms in sediments of the Pearl River estuary and vicinity. PhD thesis, The Hong Kong University.

Huang, Z. and **Zong, Y.** 1982: Grain size parameters and sedimentary facies of the Quaternary sequences in the Zhujiang (Pearl) Delta, China. *Tropical Geography* 2, 82–90 (in Chinese).

Huang, Z., Li, P., Zhang, Z., Li, K. and **Qiao, P.** 1982: *Zhujiang (Pearl) Delta*. General Scientific Press (in Chinese).

Huang, Z., Zong, Y. and **He, R.** 1985: On the depositional facies of the Zhujiang (Pearl) Delta based on fossil diatoms. *Acta Oceanologica Sinica* 7, 744–50 (in Chinese).

Huang, Z., Zong, Y. and **Zhang, W.** 2004: Coastal inundation due to sea level rise in the Pearl River Delta, China. *Natural Hazards* 33, 247–64.

Jin, D., Cheng, X., Lin, Z. and **Liu, X.** 1982: *Marine diatoms in China*. China Ocean Press (in Chinese).

Li, C., Chen, Q., Zhang, J., Yang, S. and **Fan, D.** 2000: Stratigraphy and paleoenvironmental changes in the Yangtze Delta during the Late Quaternary. *Journal of Asian Earth Sciences* 18, 453–69.

Li, P., Qiao, P., Zheng, H., Fang, G. and **Huang, G.** 1990: *The environmental evolution of the Pearl River Delta in the last 10,000 years*. China Ocean Press (in Chinese).

Nguyen, V.L., Ta, T.K.O. and **Tateishi, M.** 2000: Late Holocene depositional environments and coastal evolution of the Mekong River Delta, Southern Vietnam. *Journal of Asian Earth Sciences* 18, 427–39.

Owen, R.B. 2005: Modern fine-grained sedimentation – spatial variability and environmental controls on an inner pericontinental shelf, Hong Kong. *Marine Geology* 214, 1–26.

Palmer, A.J.M. and **Abbott, W.H.** 1986: Diatoms as indicators of sea-level change. In van de Plassche, O., editor, *Sea-level research: a manual for the collection and evaluation of data*. Geo Books, 457–88.

Raymond, P. and **Bauer, J.E.** 2001: Riverine export of aged terrestrial organic matter to the North Atlantic Ocean. *Nature* 409, 497–500.

Ruddle, K. and **Zhong, G.** 1988: *Integrated agriculture-aquaculture in south China: the dike-pond system of the Zhujiang Delta*. Cambridge University Press.

Saito, Y., Yang, Z. and **Hori, K.** 2001: The Huanghe (Yellow River) and Changjiang (Yangtze River) deltas: a review on their characteristics, evolution and sediment discharge during the Holocene. *Geomorphology* 41, 219–31.

Southon, J., Kashgarian, M., Fontugne, M., Metivier, B. and **Yim, W.W.-S.** 2002: Marine reservoir corrections for the Indian Ocean and Southeast Asia. *Radiocarbon* 44, 167–80.

Stanley, D.J. and **Warne, A.G.** 1994: Worldwide initiation of Holocene marine deltas by deceleration of sea-level rise. *Science* 265, 228–31.

Stuiver, M., Reimer, P.J. and **Braziunas, T.F.** 1998: High-precision radiocarbon age calibration for terrestrial and marine samples. *Radiocarbon* 40, 1127–51.

Ta, T.K.O., Nguyen, V.L., Tateishi, M., Kobayashi, I., Tanabe, S. and **Saito, Y.** 2002: Holocene delta evolution and sediment discharge of the Mekong River, south Vietnam. *Quaternary Science Reviews* 21, 1807–19.

Tanabe, S., Saito, Y., Sato, Y., Suzuki, Y., Sinsakul, S., Tiyapairach, S. and **Chaimanee, N.** 2003: Stratigraphy and Holocene evolution of the mud-dominated Chao Phraya delta, Thailand. *Quaternary Science Reviews* 22, 789–807.

Tanabe, S., Saito, Y., Vu, Q.L., Hanebuth, T.J.J., Ngo, Q.L. and **Kitamura, A.** 2006: Holocene evolution of the Song Hong (Red River) delta system, northern Vietnam. *Sedimentary Geology* 187, 29–61.

Van der Werff, H. and **Huls, H.** 1958–66: *Diatomeeënflora van Nederland*. 8 parts, published privately by van der Werff.

Wang, Y., Cheng, H., Edwards, R.L., He, Y., Kong, X., An, Z., Wu, J., Kelly, M.J., Dykoski, C.A. and **Li, X.** 2005: The Holocene Asian monsoon: links to solar changes and North Atlantic climate. *Science* 308, 854–57.

Woodroffe, C.D. 2000: Deltaic and estuarine environments and their late Quaternary dynamics on the Sunda and Sahul shelves. *Journal of Asian Earth Sciences* 18, 393–413.

Woodroffe, C.D, Nicholls, R.J., Saito, Y., Chen, Z. and **Goodbred, S.** 2006: Landscape variability and the response of Asian megadeltas

to environmental change. In Harvey, N., editor, *Global change and integrated coastal management*. Springer, 277–314.

Wu, C.Y., Ren, J., Bao, Y., Lei, Y.P. and **Shi, H.Y.** 2007: A long-term morphological modelling study on the evolution of the Pearl River delta, network system, and estuarine bays since 6000 yr B.P. In Harff, J., Hay, W. and Tetzlaff, D.M., editors, *Coastline changes, interrelation of climate change and geological processes*. Geological Society of America Special Paper 426, 199–214.

Xu, J., Li, Y., Cai, F. and **Chen, Q.** 1985: *The morphology of the Pearl River estuary*. China Ocean Press.

Yim, W.W.-S. 1994: Offshore Quaternary sediments and their engineering significance in Hong Kong. *Engineering Geology* 37, 31–50.

Yim, W.W.-S., Huang, G., Fontugne, M.R., Hale, R.E., Paterne, M., Pirazzoli, P.A. and **Ridley Thomas, W.N.** 2006: Postglacial sea-level changes in the northern South China Sea continental shelf: evidence for a post-8200 calendar year meltwater pulse. *Quaternary International* 145/146, 55–67.

Zhang, S., Lu, X.X., Higgitt, D.L., Chen, C-.T.A., Han, J. and **Sun, H.** 2008: Recent changes of water discharge and sediment load in the Zhujiang (Pearl River) basin, China. *Global and Planetary Change* 60, 365–80.

Zheng, Z., Deng, Y., Zhang, H., Yu, R. and **Chen, Z.** 2003: Holocene environmental changes in the tropical and subtropical areas of South China and the related human activities. *Quaternary Sciences* 24, 387–93.

Zong, Y. 1989: On depositional cycles and geomorphological development of the Han River Delta of South China. *Zeitschrift fur Geomophologie Neues Funde* 73, 33–48.

—— 1992: Postglacial stratigraphy and sea-level changes in the Han River Delta, China. *Journal of Coastal Research* 8, 1–28.

—— 2004: Mid-Holocene sea-level highstand along the southeast coast of China. *Quaternary International* 117, 55–67.

Zong, Y., Lloyd, J.M., Leng, M.J., Yim, W.W.-S. and **Huang, G.** 2006: Reconstruction of Holocene monsoon history from the Pearl River estuary, southern China, using diatoms and carbon isotope ratios. *The Holocene* 16, 251–63.

Zong, Y., Yim, W.W.-S., Yu, F. and **Huang, G.** 2009: Later Quaternary environmental changes in the Pearl River mouth region, China. *Quaternary International* in press.